



# Role of powder handling on resulting impurities in ZnSe-doped As-S-Se composite materials

ALEXANDROS KOSTOGIANNES,<sup>1,\*</sup> RASHI SHARMA,<sup>2</sup> ANDREW HOWE,<sup>2</sup> MATTHIEU CHAZOT,<sup>2</sup> MYUNGKOO KANG,<sup>2</sup> JUSTIN COOK,<sup>2</sup> KENNETH SCHEPLER,<sup>2</sup>  AND KATHLEEN A. RICHARDSON<sup>1</sup>

<sup>1</sup>CREOL, Department of Materials Science and Engineering, University of Central Florida, 4304 Scorpius St., Orlando, FL 32816, USA

<sup>2</sup>CREOL, College of Optics and Photonics, University of Central Florida, 4304 Scorpius St., Orlando, FL 32816, USA

\*[akostogiannes@Knights.ucf.edu](mailto:akostogiannes@Knights.ucf.edu)

**Abstract:** Optical composite materials made by powder processing routes can suffer from unwanted absorption loss introduced through powder handling. This can be due to impurities that are introduced during different stages of a powder processing protocol such as mixing, sieving, or grinding. The present work has evaluated the prevalence of impurities imparted to powders used to create an optical composite comprised of an As-S-Se chalcogenide base glass and ZnSe powders. The goal of this study was to identify a suitable powder handling protocol that demonstrates control of the starting particle sizes of the refractive index matched glass matrix and dopant ZnSe to acceptable levels and minimizes adverse impurities that can create loss in a glass-ceramic composite preform and envisioned fiber preforms, and fibers formed from them. Employing a heat treatment step under vacuum prior to re-melting glass powders was shown to reduce the concentration of key impurities, OH-, S-H, and Se-H, by 45.0%, 31.1% and 21.2%, respectively, as compared to re-melted material made from powders without specialized handling.

© 2022 Optica Publishing Group under the terms of the [Optica Open Access Publishing Agreement](#)

## 1. Introduction

Glass has been recognized for centuries for its ability to transmit light, particularly in the visible spectral region. Technological advancements require materials capable of transmitting light in other regions of the electromagnetic (EM) spectrum such as the infrared (IR). In this spectral region, heavy metal oxides (HMOs) or chalcogenide glasses (ChGs) may be suitable as transparent glass matrices, but HMO's typically start absorbing due to fundamental network bond resonances of the M-O bonds, in the 4-5  $\mu\text{m}$  range. Active fiber optics that operate in the mid-IR spectral region (defined as 3-5  $\mu\text{m}$  for this study) are based on host matrix materials of ChGs or fluorides (ZBLAN), combined with divalent transition metal ( $\text{TM}^{2+}$ ) ions or trivalent rare earth ( $\text{RE}^{3+}$ ) ions which can exhibit emission in the mid-IR spectral region of interest [1,2]. Here the dopant species can be present as an ion in the parent glass matrix, or in a crystalline host where particles of the dopant crystallite can be blended into a glass matrix to form an optical composite. Fabrication of a high purity optical composite fiber must meet a multitude of complex requirements. One is the prevention of absorption-inducing contamination during the composite fabrication processes, this topic forms the motivation for the present work.

Mid-IR emitting materials have been reported to have applications in fiber laser sources for precision surgery, chemical sensing and in other specialized laser systems [1-5]. Most notably, high transmission in the atmosphere of infrared light between 3  $\mu\text{m}$  and 5  $\mu\text{m}$  allowed for the development of specialized laser systems used to blind the "eyes" of heatseeking missiles [1]. The mid-IR transmission window also allows for communication of information using laser emissions through the atmosphere [3].

To create mid-IR emitting materials, one can dope either RE<sup>3+</sup> ions (such as Er<sup>3+</sup>, Dy<sup>3+</sup>, and Pr<sup>3+</sup>) or TM<sup>2+</sup> ions (such as Cr<sup>2+</sup>, Co<sup>2+</sup>, and Fe<sup>2+</sup>) into a transparent matrix (host) of the fiber core [1,6]. Most active solid-state media for fibers are based on glass matrices which can easily be drawn into fibers [1], as compared to crystalline media which while being able to be formed into fiber, are typically finite in size or optical quality [7,8]. Additionally, progress has been made in the past decade on fibers with solid crystalline cores [9].

Non-centrosymmetric tetrahedral sites in the crystalline zinc-blende structures found in ZnS or ZnSe, stabilize desirable optical transitions creating strong absorption and emission bands for transition metals when integrated into appropriate hosts [1]. Incorporation of TM<sup>2+</sup> crystals into a glass host has become an attractive method for creating mid-IR emitting composites [10,11,12]. However, these prior efforts have shown there are remaining challenges to this approach. These applications, current opportunities and limitations have been recently reviewed in [12] demonstrating the challenges of current IR fiber laser sources beyond the well-studied 2 μm regime. Of specific issue for the mid-IR region extending beyond 5 μm is the choice of host. First, glass hosts based on conventional oxide-based glass formers such as SiO<sub>2</sub>, B<sub>2</sub>O<sub>3</sub> and even TeO<sub>2</sub> cannot be used for applications of mid-IR emission or transmission in this region as their fundamental glass former metal-oxygen (M-O) bonds strongly absorb in this region of the infrared [1]. Second, the fabrication of glass plus crystallites to form homogeneous, well dispersed, low loss composites, possesses additional challenges leading to other issues. The addition of such crystallite additives to the glass matrix can result in a reduction of glass stability against crystallization, an undesirable attribute if the matrix if it is to be formed into a preform and subsequently drawn into a fiber.

Typically, composites are made to enhance physical or mechanical properties, but can also be used to create unique optical functions in optical composites. For example, it has been shown that Fe<sup>2+</sup>:ZnSe crystals can be incorporated into a suitable ChG glass matrix which allows for emission of infrared light in the 3-5 μm region [13,14]. Composites that blend a crystalline phase with a glass matrix of this type are typically made by one of two methods: internal crystal growth, or external crystallite embedding [11,15,16]. The former takes advantage of the fact that a glass is a metastable material that can crystallize under proper conditions leading in some case to agglomeration-free, homogeneously dispersed crystallites in a glass matrix [15]. While this is an attractive approach, one must have the ability to precisely control nucleation and growth of the *desired* optically active crystal phase, a process typically done via thermal treatment of the post-formed glass. Often, a secondary phase, not desirable with unwanted scatter due to agglomeration or absorption, can make this approach difficult to scale. Currently, determining the experimental procedures for internal crystal growth methods on multicomponent glasses are based on trial-and-error approaches [15]. A second approach employs physical dispersion of the crystalline phase in the glass matrix, a strategy that offers multiple choices of unique crystal/glass host combinations and is experimentally easier to control. Requirements for this approach employing a secondary 'external' crystallite embedding route includes: 1) avoidance of dissolution between dopant crystallites and glass matrix, 2) minimizing agglomeration of dopant crystals during the melting process, 3) matching refractive indices between the crystals and glass to minimize scattering losses [15] and perhaps most importantly, 4) control of the host matrix viscosity during re-melt to spatially inhomogeneous dispersion of particles to avoid segregation of particles (settling) in the composite (preform) prior to quenching/annealing. Prior efforts by others have investigated embedding TM-doped ZnSe micro-crystals into a ChG glass matrix [6,11,17]. However, none of these reports have discussed the subtleties of powder preparation and handling in the processing of both the matrix, and dopant particles and how handling of the powders during processing of the composite defines the resulting optical quality (scatter and absorption loss) of the final composite. This paper attempts to highlight these issues in the creation of mid-IR composites for potential use as fiber composites.

As noted above, glass host materials used for mid-IR or short-wave-IR optically active materials are typically made from either oxide or non-oxide (ChG) sources [1]. Typical oxide-based glasses will quench emission below 3.5  $\mu\text{m}$  due to their fast multi-phonon relaxation [1]. ChG glasses based on group VI chalcogen species (S, Se, and Te) are comprised of heavier constituent elements making vibrational frequencies of metal-chalcogen bonds very low; this leads to extremely low phonon energies which makes them viable candidates as hosts for doped crystallites capable of emitting light at wavelengths beyond 3.5  $\mu\text{m}$  [1,18].

Absorption in the parent matrix glass due to unwanted impurities in the excitation and emission bands (2-5  $\mu\text{m}$ ) must be minimized so that pump light can reach the active dopant ion and emitted light, can escape the material. Absorption bands in these regions primarily come from unwanted species related to moisture or hydrides such as -OH, -H<sub>2</sub>O, -SH, Se-H, H<sub>2</sub>Se, H<sub>2</sub>S, CO<sub>2</sub> or in the case of embedded crystallites in the glass matrix, from the dissolution of ZnSe in the chalcogenide glass matrix during the melting process [13,19–22]. Adsorbed impurities come primarily from the environment that the glass powders are kept and handled in, or from the raw materials themselves. Elemental metal pieces and powders and ChG crystalline powders such as those used in this study as well as post-melted glass powders are extremely hygroscopic, such that exposure of the precursor powders to an uncontrolled environment (air) can cause water to adsorb in large quantities. Though ChG glasses have multiple advantages as mid-IR emitting materials, they can be hindered by high concentrations of these impurities in starting elemental materials [1,15,21]. These impurities can participate in side reactions during the melting process to form species with specific absorption bands in the transparency window of interest [18,19]. In particular, the presence of H<sub>2</sub>O, OH, S-H and Se-H will have detrimental effects on lasing due to their strong absorption bands at about 2.77  $\mu\text{m}$ , 2.90  $\mu\text{m}$ , 4.02  $\mu\text{m}$ , and 4.30  $\mu\text{m}$ , respectively [18,19]. Purification techniques such as oxide volatilization, melting over hydride and oxide getters, or distillation are required typically to remove impurities from starting materials to generate low loss optical fibers [18,22]. However, the control of the post-processing steps (grinding, sieving, and mixing of powders whereby they are exposed to ambient air) of the glass and all type of composite powders is critical to avoid or decrease any contaminant that would nullify the effort made in the previous steps of purification prior to glass synthesis.

For this reason, most storage, handling (batching, grinding, sieving, mixing), and melting, are done in dry glove boxes, and dried evacuated ampoules. Excess handling of the powders through inefficient grinding performed external to a dry glove box, as well as during other processing steps such as milling, sieving and mixing, can also introduce these impurities. To understand where such impurities come from in the multi-step process needed to make, blend and consolidate a multi-phase composite, this paper reports the basis of our study to understand this evolution, with a goal of minimizing it.

In this paper an investigation of the use of an external crystallite embedding method called the ‘grind re-melt’ technique has been made with the primary goal of tracking and minimizing adsorbed impurities during the handling of glass and crystal powders. This study examines control of glass particle sizes and discusses issues with homogeneity of embedded crystals. This study also investigates impurity concentrations among different types of grinding techniques (ball milling versus hand grinding) and proposes a method for reducing adsorbed impurities in re-melted glass-crystallite composite samples.

## 2. Experimental methods

### 2.1. Grind, re-melt technique:

Figure 1 depicts the multi-step synthetic route towards glass-crystallite optical composite fabricated by the grind-remelt technique discussed above. Each step of the fabrication protocol was examined to determine where in the process the material had the greatest exposure to impurities related to ambient laboratory atmosphere conditions (nominally, 20 °C / 78% relative

humidity). This analysis was carried out primarily on an As-S-Se  $((As_2S_3)_{94.6}(As_2Se_3)_{5.4})$  base glass (BG) with some additional protocols being carried out on a commercial ZnSe powder used to represent the ‘actual’  $Fe^{2+}:ZnSe$  dopant in our composite. The motivation for the choice of the base glass’ composition is described in [19] and was chosen with the aim to precisely match the refractive indices of the glass to that of the ZnSe crystallites to allow for large ZnSe crystal sizes, therefore avoiding preparation of nano-powders. As known, the use of nanosized materials can lead to other challenges such as significant agglomeration during powder handling and large surface areas that could further contribute to further adsorption of surface impurities. Due to the significant cost of the  $Fe^{2+}:ZnSe$  crystallites, the commercial ZnSe served as a surrogate for the purpose of this study on impurities, even though the ‘intrinsic’ purity of the commercial medium was not identical to the ultimately used,  $Fe^{2+}:ZnSe$ . The parent chalcogenide base glass (BG) matrix was fabricated using a melt-quench technique from high purity (5N) elemental S, Se, and As (from Alfa-Aesar), using methods described in [19]. Elemental starting materials were stored inside a nitrogen purged MBraun glovebox that operates under an atmosphere with levels of  $H_2O < 1$  ppm and  $O_2 < 0.1$  ppm and a nominal temperature of 27 °C, prior to the melt. Starting materials were weighed and batched into quartz ampoules that had been previously cleaned with buffered HF (Alfa Aesar) and dried in a Mellen tube furnace at 392 °C for at least 2 hours. Batching of elemental materials into the cleaned quartz tubes was performed inside the same glovebox and then flame sealed under dynamic vacuum operating at approximately  $10^{-2}$  torr using an oxy-hydrogen torch. The sealed ampoules were then placed in a rocking furnace and heated at 1 °C per minute to a temperature of 750 °C with a dwell time of 14 hours. After the dwell, rocking was stopped, and the temperature was lowered to 600 °C and the tube was then removed from the furnace and quenched in air. The quenched rod was then annealed at 190 °C for 5 hours to relieve stress. Next, the base glass rod was removed from the ampoule and ground to a powder using either a porcelain mortar pestle (hand milled) inside a glovebox or a planetary ball mill operating within tungsten carbide (WC) jars with WC balls. The WC jar and balls were stored inside the glovebox between use because powders form a thin layer (pad) of powders on the walls of the jars and thus can adsorb water if left open to the atmosphere. The planetary ball mill was set up to operate with fourteen 10 mm balls for 2 hours with a rotation of 350 RPM. The ground base glass particles were removed from the jars or mortar and were separated using a sieve shaker (DuraTap Sieve Shaker, Advantech) with multiple sieves of decreasing sieve sizes (125, 53, and 25  $\mu m$ ) to obtain the desired particle sizes of  $< 25 \mu m$ . This sieve shaker operated inside a separate MBraun glovebox of equivalent environment which also stores the glass powder. Commercial ZnSe particles were then weighed and mixed with the base glass particles ( $< 25 \mu m$ ) at a loading level of 5 wt% to prepare representative 4 g composite samples. This mixture was loaded into another pre-cleaned and dried quartz ampoule and connected to dynamic vacuum ( $\sim 10^{-2}$  torr). A custom-built furnace was placed around the ampoule loaded with powders while still under vacuum and heated to a temperature of 150 °C for 1 hour to perform a “bake-off” of any surface adsorbed impurities present on the mixture powder surfaces. After the heat treatment finished, the ampoule was flame sealed and placed in a rocking furnace. The temperature was raised to 650 °C at a ramp of 1.7 °C per minute and held for a 4 hour dwell time. After the dwell time finished, the ampoule was immediately taken out of the furnace and quenched by air, then annealed at 190 °C for 5 hours. Composite samples were then removed from the ampoules and cut into slices approximately 2.5 mm thick using a Buhler Isomet slow speed saw that operated with iso-cut fluid for lubrication. These samples were then polished down to a thickness of approximately 2.0 mm using a Buehler Eco-Met 250 grinder-polisher that utilizes water for lubrication. All polished samples were cleaned well with acetone to remove residual adhesive from the polishing process.

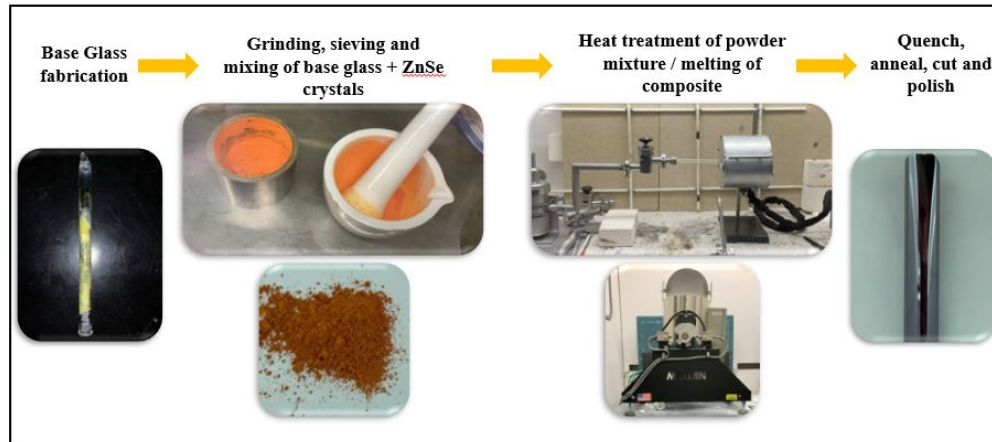


**Fig. 1.** Flow chart of the grind re-melt synthesis route for fabrication of glass + crystal composite

## 2.2. Particle size characterization

After the parent glass matrix had been batched, melted, quenched, and annealed it was removed from the quartz ampoule. As noted above, base glass was broken into powder ( $< 25 \mu\text{m}$  size) by either hand grinding or ball milling, where both processes were carried out in a controlled (dry) atmosphere. Prior to the remelt step carried out on base glass plus ZnSe mixtures, a small portion of the powders were taken to perform particle size analysis. The purpose of this experiment was to evaluate the outcome of our sieving process, with the goal of matching the size of the glass and ZnSe prior to remelt, with the aim towards enhanced homogenization during remelt. Powders were suspended in ethanol solvent and placed in a sonicator to break up any agglomerates that formed due to static effects. A few (1-2) drops of the solution was placed on a glass slide to be viewed using a white light interferometer (WLI) [23] under 20X zoom for particle size analysis. Multiple areas representative of particle dispersion/agglomeration were imaged to obtain representative information on particle dispersion, and images were captured over large areas ( $\sim 208 \mu\text{m}^2$ ). ImageJ software was used to determine the glass matrix particle size distribution by measuring the longest length of each particle/agglomerate on three micrographs. Error of the method was determined to be  $\pm 0.5 \mu\text{m}$  as referenced by finding the average particle size of commercial ZnSe powder with a known particle size ( $10 \mu\text{m}$ ).

## 2.3. Absorption characteristics of base glass and composite

Infrared spectroscopy was used to measure the impurity levels after the initial preparation of the BG and following the second re-melt step of BG plus ZnSe. Fourier transform infrared (FTIR) transmission data was recorded using a FTIR spectrometer with a spectral resolution of  $4 \text{ cm}^{-1}$ , collecting 32 accumulations [24]. Single melt base glass and re-melted composite samples were measured for IR absorption on polished bulk coupons.

## 3. Results and discussion

Resulting data from the above powder metrology characterization methods were compiled and summarized to define how each handling step in the composite synthesis led to changes or increases in the infrared absorption attributable to adsorbed moisture/oxygen-related impurities.

### 3.1. Optical microscopy analysis via white light interferometry (WLI)

The size of the glass matrix particles milled prior to the re-melt is of high importance when generating a low loss composite fiber. Base glass particles should be of similar size to the added active crystallites (in the present study, the commercially bought ZnSe powders) to prevent their agglomeration; this approach aimed to increase homogenization during re-melt. For this study, it was determined that the glass matrix particles should not exceed 25  $\mu\text{m}$ , and hence, only particles that passed this sieve size were used in the study. Figure 2 A and B show two representative micrographs (collected over areas of 208  $\mu\text{m}$  x 208  $\mu\text{m}$ ) of the powders prepared by ball milling (A) and powders prepared by hand milling (B) stitched together to evaluate the ability for the sieves to separate the glass particles to the desired size of <25  $\mu\text{m}$ . Although the two reported micrographs show some evidence of particle agglomeration, the mean particle size was found to be 7.71  $\mu\text{m} \pm 0.5 \mu\text{m}$  for ball milled glass and 12.7  $\mu\text{m} \pm 0.5 \mu\text{m}$  for hand milled glass. The two histograms shown below each micrograph in Fig. 2 represents the particle size distribution obtained from micrographs measured for the ball milled powder and hand milled powders, respectively. For the ball milled powders, nearly all measured particles are found to have their longest length to be <25  $\mu\text{m}$ , with most of the particles longest length was less than 10  $\mu\text{m}$ . Particles reported with lengths longer than 25  $\mu\text{m}$  likely have a dimension not represented in the two-dimensional micrograph with a length shorter than 25  $\mu\text{m}$ , allowing them to pass through the sieve. Hand milled powders were observed to have a larger number of particles with sizes >25  $\mu\text{m}$ , indicating they have a morphology of longer platelets compared to the ball mill powders, or something in their handling led to further agglomeration post-sieving. The error of this method may skew the observed base glass particle size to slightly larger sizes than are present after sieving. Nevertheless, these results confirm that grinding using the ball milling procedure will more readily produce a smaller average particle size and that the sieving procedure used will generate base glass powders with acceptable sizes using either method.

### 3.2. Infrared absorption spectroscopy

The purpose of using infrared spectroscopy was to identify and quantify impurities found in single and re-melted glass samples within the spectral region of interest (2.5– 5.0  $\mu\text{m}$ ) though impurities (such as arsenic oxides) may be located at longer wavelengths. The powder handling protocol described in this paper has multiple steps of handling that have the potential for introducing impurities into our base glass powders that carry over into the re-melted product. Handling here refers to all steps that require manipulation of powders such as grinding, sieving, batching, and mixing, prior to introduction of the batch into the ampoule. No elemental purification was done to remove the intrinsic impurities of C, H, or O that are present in the as-purchased As, S, or Se as it was beyond the scope of this report. To create an optical fiber with minimal loss however, a purification of these elements would likely be necessary.

Table 1 provides a summary of all sample types that were investigated by infrared absorption spectroscopy. Four variables were under investigation including the effect of methods for pulverizing the base glass (ball milled / hand milled), sizing the powders once ground via sieving, mixing of the glass and crystallite ZnSe powders (by hand) and the use of a heat treatment on powders before re-melt.

Figure 3 shows the infrared absorption spectra of re-melted base glasses made by either ball milling or hand milling with a parent base glass (BG) for reference. Hand grinding with a porcelain mortar pestle was shown to have less impact on absorption than ball milling with tungsten carbide jars and balls. This figure also shows that impurities are likely picked up by the powders regardless of how they are handled using either of the grinding methods. Milling the bulk base glass by hand ultimately introduced less impurities in the form of hydrides and moisture, than ball milling. This is likely because the ball mill operated outside of the glovebox while the mortar pestle was handled inside the glovebox. Although the powders were loaded

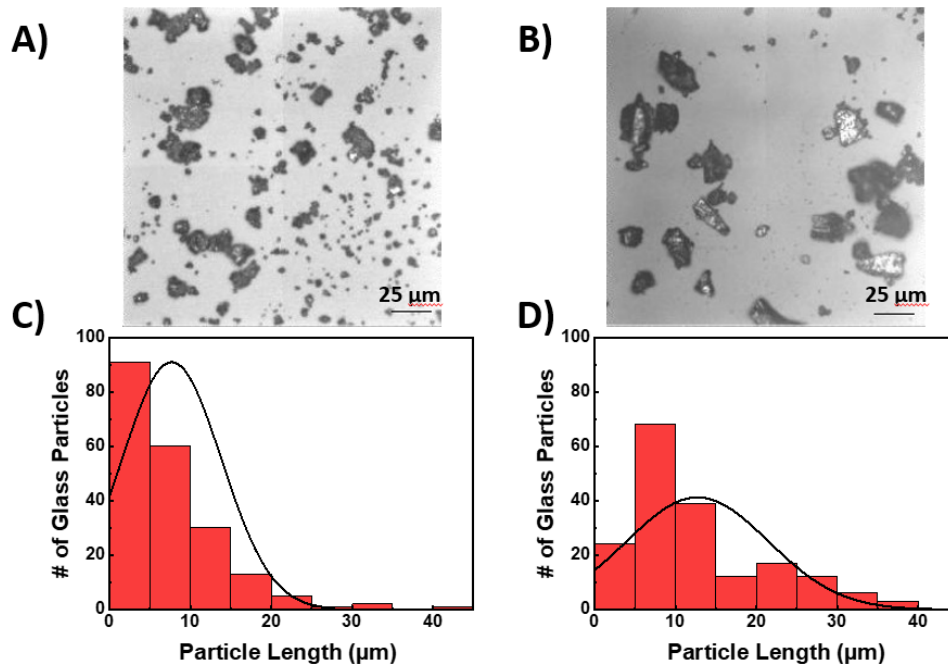


**Fig. 2.** Representative optical micrographs of base glass powders pulverized by either ball milling (A) or hand milling (B) taken with a WLI imaging instrument under 20X zoom; Particle size distribution of ground base glass particles using ball milling (C) or hand milling (D)

**Table 1. Summary of materials and their respective method for preparation. All four samples were evaluated using Infrared transmission / absorption spectroscopy**

Sample type	Key variable	Desired information
Single melt	Reference	Baseline for re-melts
Ground powder	Before sieving/ After sieving	Impurities adsorbed from sieving
Re-melted	Ball milled / Hand milled	Determine best milling method
Re-melted	With or Without Heat Treatment	Reduction of contamination
Re-melted	With ZnSe crystals	Impact of micro crystals

into the WC jars inside the glovebox (in a dry  $N_2$  atmosphere) air could have leaked inside the jar during the milling process. Additionally, the jars and balls were not baked out prior to use. However, grinding large masses of powders with a mortar pestle is not a viable option for fabrication outside of a small melt, laboratory setting. Therefore, making improvements to the ball milling process (such as milling within a controlled atmosphere) is a viable route for future work. The hand-milled re-melted base glass also contained absorptions located at  $3.41 \mu\text{m}$  and  $3.52 \mu\text{m}$  that were due to residual adhesive from polishing that was clearly not completely removed despite cleaning; note that this residue was not able to be removed using our current cleaning protocol and is not intrinsic to the material. This suggests further enhancement to cleaning methodology should also be carried out to reduce these losses. Figure 4 shows two absorption spectra that represent an effective method for removing adsorbed impurities from handling. For this study, we subjected the batch prior to remelt to a ‘dynamic’ heat treatment of  $150 \text{ }^\circ\text{C}$  for 1 hour under dynamic vacuum prior to sealing the ampoule for re-melt.

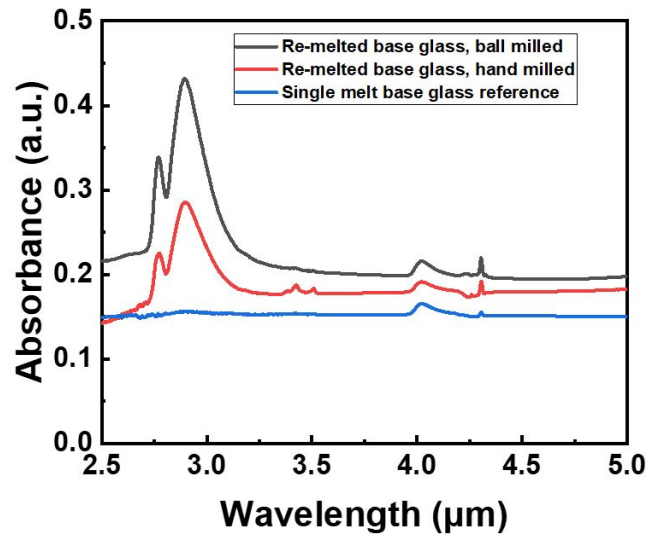


**Fig. 3.** Comparison of IR absorbance spectra of re-melted base glass that was ground using either mortar pestle ( $t = 1.78$  mm) or planetary ball mill (1.76 mm) with single melt base glass as reference ( $t = 1.90$  mm); not corrected for thickness or Fresnel loss

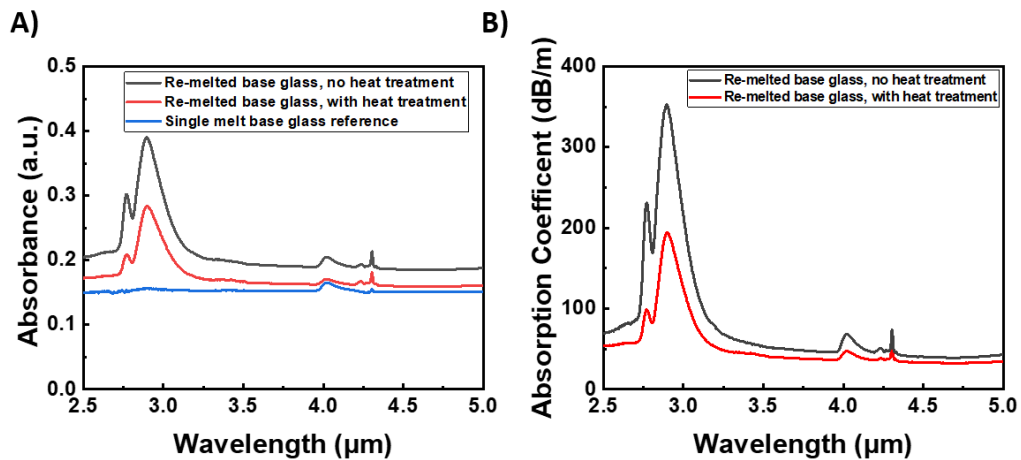


**Fig. 4.** A, absorbance spectra of re-melted glass matrix without (grey,  $t = 1.76$  mm) and with (red,  $t = 1.78$  mm) a heat treatment of  $150^{\circ}\text{C}$  for 1 hour under dynamic vacuum; shown for comparison is data for the single melt base glass as a reference ( $t = 1.90$  mm); spectra are not corrected for thickness or Fresnel reflections. B, absorption coefficient of both samples in left, used for calculations of impurities

As can be seen, this step lowered the concentration of impurities present in re-melted base glass. Figure 4 also presents the plot of absorbance coefficient for the re-melted coupons made with a pre-heat treatment step and without the pre-heat treatment step. The values from the absorbance maxima were used to quantify the concentration of impurities in the 2.5–5  $\mu\text{m}$  region. This calculation was done by first calculating absorption coefficient,  $\alpha$  ( $\text{cm}^{-1}$ ), which was derived from Fresnel's formula [18]. For a sample with a thickness  $t$ , absorption coefficient can be calculated with transmission data with Beer-Lambert's law using the equation:

$$T = \frac{(1 - R)^2}{(1 - R^2)} e^{-\alpha t} \quad (1)$$

Where  $T$  is the transmission of a bulk sample and  $R$  is the reflection coefficient given by the equation:

$$R = \frac{(n - 1)^2}{(n + 1)^2} \quad (2)$$

with  $n$  being the refractive index of the glass [18]. The refractive index of the sample was measured at five wavelengths (1.9  $\mu\text{m}$ , 3.3  $\mu\text{m}$ , 4.0  $\mu\text{m}$ , 4.5  $\mu\text{m}$ , and 5.25  $\mu\text{m}$ ) using a modified Metricon instrument [25]. The refractive indices were fitted using the Sellmeier equation, and a dispersion curve was derived through-out the region of interest [19]. The procedure followed for this derivation can be found in [26].

To quantify the concentration of an impurity, the following relationship between absorption ( $\alpha$ ) and extinction coefficient ( $\epsilon$ ) can be used:

$$[\text{Impurity}] = \frac{\alpha(\text{dB/m})}{\epsilon(\text{dB/m})} \quad (3)$$

Literature values of the extinction coefficients for -OH, SH, and Se-H impurities can be seen in Table 2 along with the calculated absorption coefficients and concentrations in ppm [18,21,22] along with data from our materials. The observed absorption bands correspond to the vibrational modes of  $\text{H}_2\text{O}$  at 2.77  $\mu\text{m}$ ;  $-\text{O}-\text{H}^-$  at 2.90  $\mu\text{m}$ ;  $-\text{S}-\text{H}^-$  at 4.02  $\mu\text{m}$ ;  $\text{CO}_2$  at 4.23  $\mu\text{m}$ ; and Se-H at 4.30  $\mu\text{m}$  [18,21,22].

**Table 2. Relevant impurity concentrations of re-melted glass matrix with and without a pre-heat treatment process of 150 °C for 1 hour under dynamic vacuum**

Impurity	Position of the maximum of the absorption band ( $\mu\text{m}$ )	Extinction Coefficient, $\epsilon$ (dB/m · ppm)	Base glass without heat treatment of powders		Base glass with heat treatment of powders	
			$\alpha$ (dB/m)	[Impurity] ppm	$\alpha$ (dB/m)	[Impurity] ppm
$\text{H}_2\text{O}$	2.77	-	231	-	98.5	-
OH	2.90	5.0	353	70.6	194	38.8
SH	4.02	2.5	68.3	27.3	47.1	18.8
$\text{CO}_2$	4.23	-	50.4	-	38.5	-
Se-H	4.30	1.00	74.0	74.0	58.3	58.3

The largest and most problematic impurity band seen in all spectra is -OH which arises at 2.90  $\mu\text{m}$ . Utilization of the heat treatment protocol prior to re-melting glass powders reduced the concentration of key impurities, OH-, S-H, and Se-H, by 45.0%, 31.1% and 21.2% respectively. These percentages were obtained by taking one minus the ratio of the impurity concentration of

the heat-treated base glass and the impurity concentration of the non heat-treated base glass.

$$\%Impurity = \left(1 - \left(\frac{[impurity]_{Heat-treated}}{[impurity]_{Unheat-treated}}\right)\right) \times 100 \quad (4)$$

To compare our data to that found in other studies, previous studies have shown that other purification protocols can be implemented to significantly reduce the concentration of impurities found in similar chalcogenide composite fiber materials [18,21], reducing various impurities to low ppm (few dB/m) levels. Analysis of the data on our samples show that the heat-treated sample has overall a lower level of absorption across the spectra and less intense peaks for -O-H<sup>-</sup>, -S-H<sup>-</sup> and Se-H as seen by the lower concentrations of impurities in Table 2.

The capability of lowering the concentration of water is of paramount importance to generating a composite fiber with low levels of loss. In Table 3, tabulation of all absorption bands in the single melt and re-melted glass samples shows which impurities are found in the starting elemental material and which are due to handling. The two main absorptions observed in each re-melted sample (not found in single melt) are attributed to water and hydroxide that has been adsorbed from the experimental process. Water and OH<sup>-</sup> were found to be, as expected, the strongest absorbers of light of all the impurities present in these composite materials. This is problematic as these impurity absorptions overlap with the same wavelength regions of maximum absorption of the active Fe<sup>2+</sup>:ZnSe dopant. Removal of these impurities alone would significantly increase the amount of light emitted from our fiber composites by allowing for more light to be absorbed by Fe<sup>2+</sup>: ZnSe. Absorption of the hydride contaminants that were found in our materials are less intense but will still interfere with the light emitted from our sample as these impurities will re-absorb light generated from the Fe<sup>2+</sup>: ZnSe particles before they can leave the material.

**Table 3. Spectral positions of impurities found in single melt and re-melted glass matrix samples**

Impurity	Spectral absorption position in single melt reference	Spectral absorption position in all re-melted base glass samples
H <sub>2</sub> O	-	2.77
OH	-	2.90
SH	4.02	4.02
CO <sub>2</sub>	4.23	4.23
Se-H	4.30	4.30

Figure 5 shows the impact of incorporating 5 wt% of ZnSe into the re-melted base glass. The baseline absorption significantly increases compared to the base glass only re-melts. This is likely due to the partial dissolution of ZnSe to ZnS which will cause scattering due to both formation of bubbles and a mismatch of refractive index between the undesired ZnS and glass matrix. Also, the impurity associated with -SH groups dominate in the 5 wt % composite over all other impurities observed. As all handling was identical to the re-melted base glass alone, the increased absorption peak associated to -SH is attributed directly to the addition of the commercial ZnSe powders. Purification of the base glass and commercially purchased ZnSe would be necessary to fabricate a low loss optical composite fiber, though it has been shown that emission is possible using equivalent crystallites of Fe<sup>2+</sup>: ZnSe in the same host [14].

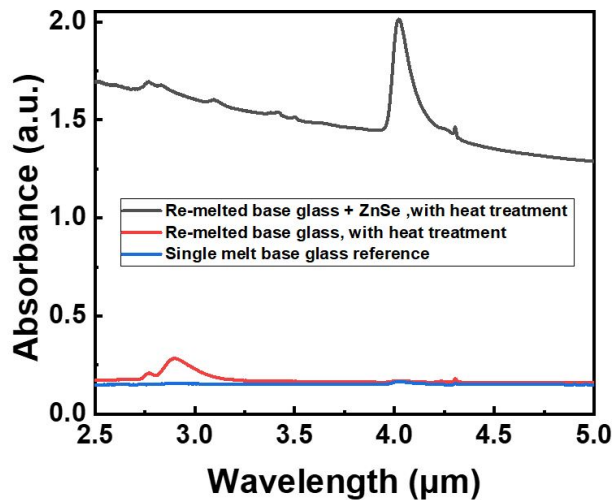


**Fig. 5.** IR absorbance spectra of base glass + 5 wt% ZnSe, with heat treatment ( $t = 1.80$  mm) and base glass alone with heat treatment ( $t = 1.78$  mm) with single melt base glass as a reference ( $t = 1.90$  mm); spectra not corrected for thickness or Fresnel reflections.

#### 4. Conclusion

To make a composite material capable of emitting light or transmitting in the mid-IR region with low amounts of loss, the handling of precursor powder materials must be carefully controlled at every step in the process to avoid addition of impurities. In this work, a composite comprised of an As-S-Se base glass powder was blended with micron size ZnSe powder to simulate a handling protocol now being used to form an active  $\text{Fe}^{2+}:\text{ZnS}$  containing, bulk composite. Our study aimed to quantify loss associated with various handling protocols to optimize powder handling procedures to understand where specifically in the fabrication process, loss-inducing absorptive species were introduced into the composite, thereby impacting the optical emission dopant  $\text{Fe}^{2+}:\text{ZnSe}$  crystals.

Optical microscopy of the post ‘grind-remelt’ bulk composite showed that the post-sieved base glass particles with targets to be  $< 25 \mu\text{m}$ , were on average  $7.71 \mu\text{m} \pm 0.5 \mu\text{m}$  while the average size of the hand milled base glass powders was  $12.7 \mu\text{m} \pm 0.5 \mu\text{m}$ . With our current technique however, ball milling was found to be the best option available in terms of efficiency but not for preventing adsorption of impurities. Removal of such extrinsic impurities by a moderate heat treatment under vacuum showed great success in its ability to remove moisture, and hydrides introduced from handling. It was found that including a “bake-off” heat treatment under vacuum before placing the glass matrix into the furnace for re-melt was able to reduce the concentration of the three key impurities, OH-, S-H, and Se-H, by 45.0%, 31.1% and 21.2% respectively. Future efforts to improve upon the work presented here could investigate the time dependency of impurity removal during the heat treatment purification of powders. Additionally, it would be interesting to apply this calcination step to similar hygroscopic glass powder systems.

**Funding.** Air Force Office of Scientific Research (FA9550-19-1-0127).

**Acknowledgments.** The author thanks the Chemistry department of the University of Central Florida (UCF) and their Undergraduate Research program, for their mentorship throughout this project. Co-authors (MC and MK) acknowledge the support of the UCF Pre-eminent Post-doctoral Program (P3).

**Disclosures.** The authors declare no conflicts of interest

**Data availability.** Data underlying the results presented in this paper are not publicly available at this time but may be obtained from the authors upon reasonable request.

## References

1. S.D. Jackson and R.K. Jain, "Fiber-based sources of coherent MIR radiation: Key advances and future prospects," *Opt. Express* **28**(21), 30964–31019 (2020).
2. X. Zhu and N. Peyghambarian, "High-power ZBLAN glass fiber lasers: review and prospect," *Adv. in OptoElectronics*, **2010**, 1–23 (2010).
3. Y. Su, W. Wang, X. Hu, H. Hu, X. Huang, Y. Wang, J. Si, X. Xie, B. Han, H. Feng, Q. Hao, G. Zhu, T. Duan, and W. Zhao, "10 Gbps DPSK transmission over free-space link in the mid-infrared," *Opt. Express* **26**(26), 34515–34528 (2018).
4. M. C. Pierce, S. D. Jackson, M. R. Dickinson, T.A. King, and P. Sloan, "Laser-tissue interaction with a continuous wave 3- $\mu\text{m}$  fiber laser: preliminary studies with soft tissue," *Lasers Surg. Med.* **26**(5), 491–495 (2000).
5. X. Zhang, B. Bureau, P. Lucas, C. Boussard-Pledel, and J. Lucas, "Glasses for seeing beyond visible," *Chem. Eur. J.* **14**(2), 432–442 (2008).
6. X. Lu, J. Li, L. Yang, J. Ren, M. Sun, A. Yang, Z. Yang, R. K. Jain, and P. Wang, "Broadband mid-infrared (2.5–5.5 $\mu\text{m}$ ) emission from  $\text{Co}^{2+}/\text{Fe}^{2+}$  co-doped chalcogenide glass ceramics," *Opt. Lett.* **45**(9), 2676–2679 (2020).
7. M. Ito, S. Hraiech, C. Goutaudier, K. Lebbou, and G. Boulon, "Growth of  $\text{Yb}^{3+}$ -doped  $\text{KY}_3\text{F}_{10}$  concentration gradient crystal fiber by laser-heated pedestal growth (LHPG) technique," *J. Cryst. Growth* **310**(1), 140–144 (2008).
8. G. Boulon, A. Collombet, A. Brenier, M. T. Cohen-Adad, A. Yoshikawa, K. Lebbou, J.H. Lee, and T. Fukuda, "Structural and spectroscopic characterization of nominal  $\text{Yb}^{3+}:\text{Ca}_8\text{La}_2(\text{PO}_4)_6\text{O}_2$  oxyapatite single crystal fibers grown by the micro-pulling-down method," *Adv. Funct. Mater.* **11**(4), 263–270 (2001).
9. F.A. Martinsen, B.K. Smeltzer, M. Nord, T. Hawins, J. Ballato, and U.J. Gibson, "Silicon-core glass fibers as microwire radial-junction solar cells," *Sci. Rep.* **4**(1), 6283–62977 (2015).
10. R.A. Mironov, E.V. Karaksina, A.O. Zabezhailov, R.M. Shaposhnikov, M.F. Churbanov, and E.M. Dianov, "Mid-IR luminescence of  $\text{Cr}^{2+}$ : II-VI crystals in chalcogenide glass fibres," *Quantum Electron.* **40**(9), 828–829 (2010).
11. E. V. Karaksina, L. A. Ketkova, M. F. Churbanov, and E. M. Dianov, "Preparation of mid-IR active  $\text{As}_2\text{S}_3/\text{ZnS}(\text{ZnSe}):\text{Cr}^{2+}$  composites," *Inorg. Mater.* **49**(3), 223–229 (2013).
12. S. Jackson, M. Bernier, and R. Vallée, *Mid-Infrared Fiber Photonics: Glass Materials, Fiber Fabrication and Processing, Laser and Nonlinear Sources* (Elsevier, 2021).
13. M. Chazot, A. Kostogiannes, M. Julian, C. Feit, J. Sosa, M. Kang, C. Blanco, V. Rodriguez, F. Adameitz, D. Verreault, P. Banerjee, K. Schepler, M. C. Richardson, and K. A. Richardson, "Enhancement of ZnSe stability during optical composite processing via Atomic Layer Deposition," *J. Non-Cryst. Solids* **576**, 121259 (2022).
14. J. Cook, M. Chazot, A. Kostogiannes, R. Sharma, C. Feit, J. Sosa, P. Banerjee, M. Richardson, K. A. Richardson, and K. L. Schepler, "Optically active  $\text{Fe}^{2+}$ -doped ZnSe particles in a chalcogenide glass matrix," *Opt. Mater. Express* **12**(4), 1555–1563 (2022).
15. J. Ren, X. Lu, C. Lin, and R. K. Jain, "Luminescent ion-doped transparent glass ceramics for mid-infrared light sources," *Opt. Express* **28**(15), 21522–21548 (2020).
16. X. Lu, Z. Lai, R. Zhang, H. Guo, J. Ren, L. Strizik, T. Wagner, G. Farrell, and P. Wang, "Ultrabroadband mid-infrared emission from  $\text{Cr}^{2+}$  doped infrared transparent chalcogenide glass ceramics embedded with thermally grown ZnS nanorods," *J. Eur. Ceram. Soc.* **39**(11), 3373–3379 (2019).
17. D. V. Martyshkin, J. T. Goldstein, V. V. Fedorov, and S. B. Mirov, "Crystalline  $\text{Cr}^{2+}:\text{ZnSe}$  chalcogenide glass composites as active mid-IR materials," *Opt. Lett.* **36**(9), 1530–1532 (2011).
18. A. Yadav, M. Kang, C. Goncalves, C. Blanco, R. Sharma, and K. Richardson, "Impact of raw material surface oxide removal on dual band infrared optical properties of  $\text{As}_2\text{Se}_3$  chalcogenide glass," *Opt. Mater. Express* **10**(9), 2274–2288 (2020).
19. M. Chazot, C. Arias, M. Kang, C. Blanco, A. Kostogiannes, J. Cook, A. Yadav, V. Rodriguez, F. Adamietz, D. Verreault, S. Danto, T. Loretz, A. Seddon, D. Furniss, K. Schepler, M. C. Richardson, and K. A. Richardson, "Investigation of ZnSe stability and dissolution behavior in As-S-Se chalcogenide glasses," *J. Non-Cryst. Solids* **555**, 120619 (2021).
20. D. Thompson, S. Danto, J. D. Musgraves, P. Wachtel, B. Giroire, and K. Richardson, "Microwave assisted synthesis of high purity  $\text{As}_2\text{Se}_3$  chalcogenide glasses," *Phys. Chem. Glasses: Eur. J. Glass Sci. Technol. B.* **54**(1), 27–34 (2013).
21. S. Danto, D. Thompson, P. Wachtel, J. D. Musgraves, K. Richardson, and B. Giroire, "A comparative study of purification routes for  $\text{As}_2\text{Se}_3$  chalcogenide glass," *Int. J. Appl. Glass Sci.* **4**(1), 31–41 (2013).
22. G. E. Snopatin, V. S. Shriyaev, V. G. Plotnichenko, E. M. Dianov, and M. F. Churbanov, "High purity chalcogenide glasses for fiber optics," *Inorg. Mater.* **45**(13), 1439–1460 (2009).
23. ZYGO Corporation, NewView 9000, Laurel Brook Rd. Middlefield Ct USA 06455
24. ThermoFisher Scientific Corporation, Nicolet Is5, 168 Third Ave. Waltham, MA USA 02451
25. Metricon Corporation, 2010, 12 North Main St. Pennington, NJ USA 08534
26. M. Kang, I. Martin, R. Sharma, C. Blanco, S. Antonov, T. J. Prosa, D. J. Larson, H. Francois-Saint-Cyr, and K. Richardson, "Unveiling true 3D nanoscale microstructural evolution in chalcogenide nanocomposites: a roadmap for advanced infrared functionality," *Adv. Opt. Mater.* **9**(9), 2002092 (2021).